Quantum electronic stability and spectroscopy of ultrathin Pb films on Si(111)7×7

A. Mans,* J. H. Dil, and A. R. H. F. Ettema
Department of Nanoscience, Delft University of Technology, Lorentzweg 1, 2628CJ Delft, The Netherlands

H. H. Weitering
Department of Physics and Astronomy, The University of Tennessee, Knoxville, Tennessee 37996
and Solid State Division, Oak Ridge National Laboratory, Oak Ridge, Tennessee 37831
(Received 5 August 2002; published 19 November 2002)

The growth of Pb on Si(111)7×7 has been studied with photoelectron spectroscopy. At low temperature (110 K), Pb grows in a quasi layer-by-layer mode that allows for the direct observation of discrete quantum well states. The quantum well states are analyzed in terms of the Bohr-Sommerfeld phase quantization model using a phenomenological phaseshift function and reduced quantum numbers. Fermi-level crossings occur when the film thickness $Nd=n(\lambda_F/2)$, where d is the atomic layer spacing and λ_F the bulk Fermi wavelength (N,n are integers). The photoemission intensity from the quantum well states shows a strong modulation with photon energy which can be interpreted on the basis of the matrix elements for direct transitions in bulk Pb(111). The in-plane effective mass of the quantum well states is greatly enhanced in the vicinity of the substrate band edge. The present results provide important elements for understanding the growth morphology of Pb films in recent STM studies.

DOI: 10.1103/PhysRevB.66.195410 PACS number(s): 79.60.Dp, 73.21.Fg, 68.55.Jk

I. INTRODUCTION

There is an increasing body of experimental evidence suggesting that the growth mode of ultrathin metal films at moderately low temperatures is significantly affected by the quantum-size effect. The earliest report dates back to 1989 when Hinch *et al.*[1] studied the growth of Pb on Cu(111) near 200 K and observed a doubling of the periodicity in the specular beam intensity in He scattering experiments during growth. They proposed that Pb grows in bilayers and noted that the bilayer periodicity is almost perfectly commensurate with half the Fermi wavelength: $Nd\approx n\lambda_F/2$. The proposed link between quantum confinement and growth mode did not survive later scrutiny[2] but recent studies convincingly showed that electronic structure, specifically quantum confinement perpendicular to the film, dictates the growth morphology during the early stages of growth at low temperature. ''Magic film thickness''[3] and ''preferred island heights''[4,5] have been observed for several metal-semiconductor interfaces. The preferred island heights of Pb on Si(111) can furthermore be tuned by tuning the confinement parameters (i.e., boundary conditions) of the film.[6] The relation between quantum confinement and structural stability was demonstrated also for metal-on-metal epitaxy in which case the confinement is not due to the absolute band gap in the substrate but rather to a relative band gap in the growth direction.

To understand and predict the morphological evolution during low-temperature growth, one needs to understand the underlying physics in detail; analysis of the quantized electronic states and their boundary conditions is therefore essential. To calculate these levels, one can start from the standard textbook example of a particle in a one-dimensional, finite square well potential. A slightly more sophisticated model—the ''electronic growth'' model[7]—explicitly addresses the role of the semiconductor substrate and revealed that ultrathin flat films can be thermodynamically stable, marginally stable, or even unstable, depending on their thickness, similar to the existence of magic numbers for metal nanoclusters.[8] The unstable films are expected to phase separate into multiple-height islands of stable thickness, provided that the temperature is high enough to allow sufficient surface diffusion. These predictions have been verified in the experimental studies cited above, but the electronic growth model is too simplistic to quantitatively reproduce the global energy minima of the metal films. Total energy calculations within the framework of density functional theory (DFT) calculations should be much more accurate but these often cannot include the (usually) incommensurate substrate. Further complications arise from the fact that the structure of the interfacial wetting layer is usually disordered or totally unknown.

To obtain more knowledge about the Pb/Si(111)7×7 system and especially about the quantized electronic states, we performed photoemission measurements as a function of layer thickness. Photoemission is a suitable technique to probe quantum well states directly. Normal emission data at fixed photon energy will show quantum well states dispersing to lower binding energy as the film thickness increases. The Bohr-Sommerfeld phase accumulation model very well reproduces this behavior and furthermore yields the interfacial phaseshift parameter. Normal emission data at different photon energies reveal strong matrix element effects for photo-ionization, and angle-dependent photoemission data reveal a large in-plane effective mass for states that are close to the Fermi energy. These experimental results have been analyzed in detail and their implications for growth and stability will be discussed in the context of recent STM studies.

II. EXPERIMENT

The experiments were performed at beamline BL 33 of the MaxLab synchrotron radiation facility in Lund, Sweden.[9]

The base pressure of the chamber was 3×10^{-11} mbar. The photon energies used were $\geqslant 22$ eV because otherwise second-order light from the monochromator would produce spurious features in the photoemission spectra. An *n*-type silicon sample was cleaned by flashing to 1375 K by resistive heating. After cooling to room temperature the sample showed a sharp 7×7 low-energy electron-diffraction (LEED) pattern and photoemission spectroscopy showed no traces of contamination. The sample was subsequently cooled by a liquid-nitrogen cold finger to 110 K. Pb was evaporated from a Knudsen cell at a source temperature of 870 K which resulted in an evaporation speed of 0.11 monolayer (ML) per minute. The growth temperature of 110 K appeared low enough to prevent the presence of preferred (magic) island heights. Pb grows in the (111) orientation on Si(111)7×7 and therefore the film thickness is given in terms of a Pb(111) monolayer (1 ML$=9.43\times10^{14}$ atoms/$\cdot$cm^{-2}).

The Pb evaporation speed was calibrated from the evolution of the Schottky barrier as a function of deposition time and from the ratio of the Pb5*d*/Si2*p* photoemission line intensities as a function of deposition time.[10] This intensity ratio abruptly saturates at the absolute coverage of 0.65 ML, which was independently checked with Rutherford backscattering spectrometry. The development of the Schottky barrier is complete at a coverage of 0.8×0.65 ML $=0.52$ ML.[10] This calibration was consistent with the readings of our quartz crystal oscillator.

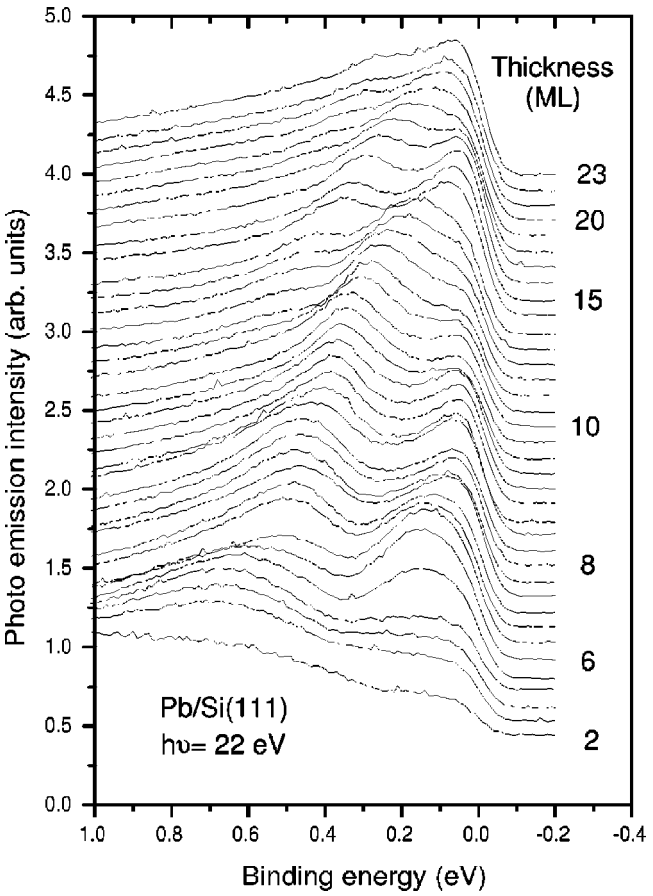

FIG. 1. Normal-emission photoemission spectra of Pb on Si(111)7×7. The coverage ranges from 2 to 23 ML.

III. RESULTS AND DISCUSSION

A. Photoemission from quantum well states

A series of photoemission spectra of Pb on Si(111)7×7 at 110 K is shown in Fig. 1. The spectra were recorded at normal emission with 22 eV photon energy. The incident angle was 45° and the polarization was in the plane of the incident photons and emitted electrons. The signature of the quantum well states is evident from (i) the binding energy shift of the peaks with increasing Pb coverage and (ii) the fact that the binding energy of a quantum well state is independent of photon energy (Fig. 6). Binding energies were determined from the minima of the second derivatives of the photoemission spectra. One can clearly see that the quantum well states shift to lower binding energy with coverage, which may seem counter intuitive but will be explained later on. At 22 eV photon energy, the quantum well states are only observed within a binding energy interval from 0 to 0.7 eV below the Fermi level.

Figure 2(a) shows a plot of the quantum well energies as a function of layer thickness (in ML Pb). As a first step towards the interpretation of the data we employ a symmetrical, one-dimensional square well potential[11] with a depth of 12.4 eV (8.1 + 4.3 eV for the Pb work function) and an effective mass of $1.2m_e$. Filled squares represent the energies of the quantum well states that are calculated with this model. The quantum numbers *n* are indicated and it can be seen that for each measured photoemission "branch" *p* $\equiv 3N-2n$ remains constant (*N* is the layer thickness in ML). The reduced quantum numbers *p* are indicated in Fig. 2(a).

Each photoemission branch has the property that it supports a new quantum well state as the thickness increases in multiples of two monolayers. The number of antinodes in the wave function increases by three for each bilayer increment, hence the condition $3N-2n=$ constant. From the bulk band structure of Pb, one finds that in this range of energy and momentum, $\lambda\approx4d/3$, which does indeed show that a bilayer of Pb can support approximately three antinodes ($d=2.85$ Å and $\lambda_F=3.95$ Å).[11] The energy goes up slightly for each bilayer increment, which is due to the fact that the wavelength must be squeezed a little so that the wave function can still fit in the well. The number *p* can be viewed as a reduced quantum number corresponding to a long-wavelength (λ') modulation which satisfies the condition $p\lambda'/2=2Nd$.

This simple model reproduces the scanning tunneling miscroscopy and spectroscopy (STM/STS) observations of Su *et al.*[5] and Altfeder *et al.*[12] that each quantum well branch has only contributions from odd- or even-numbered layers. Branches with reduced quantum number $p=$ even (odd) only have contributions from even (odd) layers. Another property of the system is that all films with an even number of atomic layers support a quantum well state 0.6 eV above the Fermi level. These states all belong to the branch $p=0$ [not shown

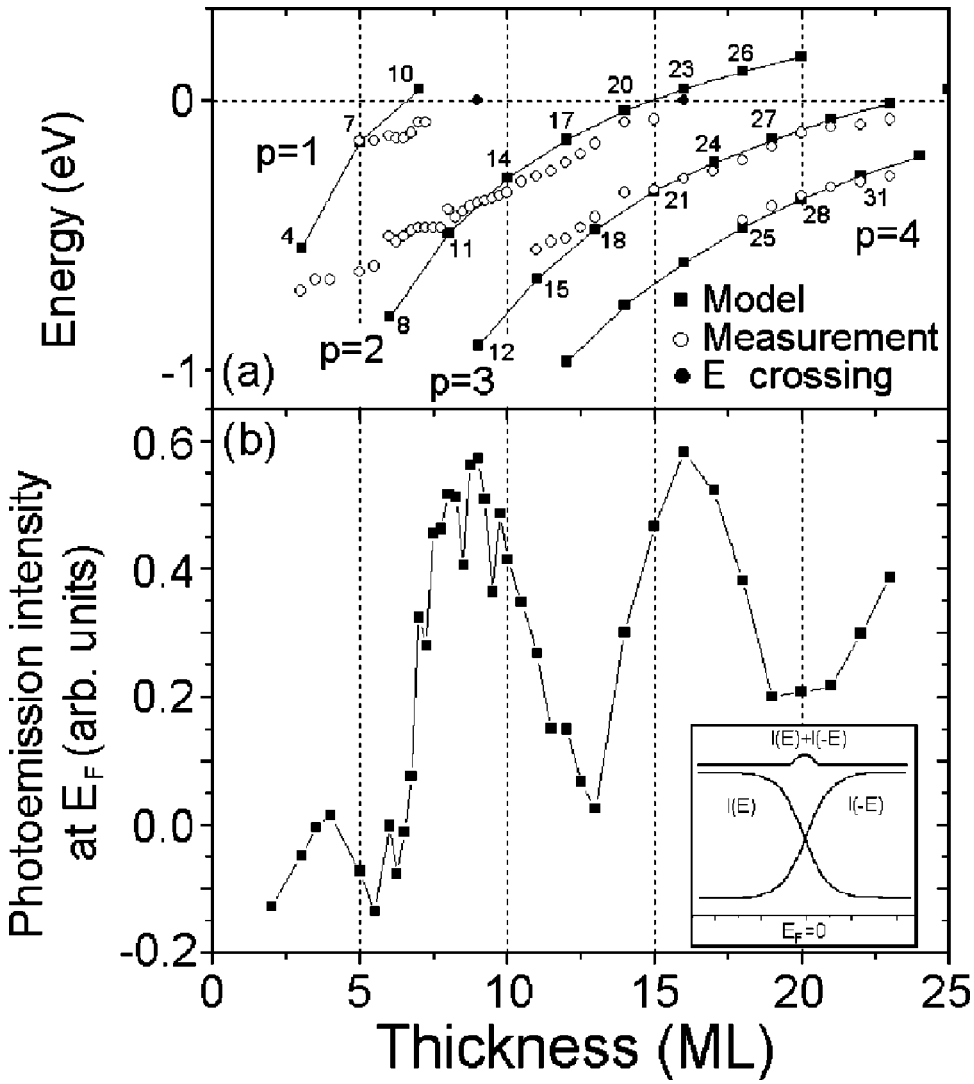

FIG. 2. (a) Open circles: experimental quantum well states as a function of Pb coverage. The filled squares represent the best fit of the one-dimensional square well model to the photoemission data. The quantum numbers n and p are indicated. The solid lines serve as a guide to the eye. (b) Photoemission intensity at the Fermi level as a function of Pb coverage. Inset: illustration of the symmetrization procedure.

in Fig. 2(a)] and have $k=3\pi/2d$ exactly at the midpoint of the second Brillouin zone.[5] Su *et al.*[5] and Altfeder *et al.*[12] performed STM/STS measurements on Pb on Si(111)7×7 at 200 K. Su *et al.* observed flat-top (magic) islands on top of a wetting layer of Pb, while Altfeder *et al.* performed their measurements on a wedge shaped Pb island on a wetting layer. They both observed the $p=0$ state in STS for island heights corresponding to an odd number of atomic layers above the wetting layer. This proves that the wetting layer in their studies consists of an odd number of Pb layers.

From the measurements it is furthermore deduced that the Pb growth is not perfectly layer-by-layer. The quantum well states disperse continuously with Pb coverage and do not reveal monolayer resolution. Neighboring quantum well states in each branch are often separated by less than 0.1 eV and hence it is also much more difficult to achieve monolayer resolution as compared with e.g., Ag films.[13] The small separation of the quantum well states is a direct consequence of the property that each bilayer supports three new states.

We now turn to the more accurate description in terms of the Bohr-Sommerfeld phase accumulation model

$$2k(E)Nd+\Phi_B(E)+\Phi_C(E)=2\pi n \qquad (1)$$

with $k(E)$ the Pb band structure in the ΓL direction (perpendicular to the surface), Nd the thickness of the well, Φ_B and Φ_C the phaseshifts at the surface-vacuum interface and the metal-semiconductor interface, respectively, and n the principal quantum number of the state. The wave vectors $k(E)$ are located in the second Brillouin zone. When we approximate the surface potential barrier with an image potential, the phaseshift at the vacuum side of the well can be approximated from the well-known WKB expression:[14]

$$\Phi_B(E)/\pi=[3.4/(E_V-E)]^{1/2}-1, \qquad (2)$$

where E_V is the vacuum level (or work function). Φ_B varies slowly as function of energy. It ranges from -0.11π at the Fermi level and -0.18π at 0.7 eV binding energy to -0.36π at 4 eV binding energy. The total phaseshift ($\Phi_B+\Phi_C$) and $k(E)$ can be determined from the experiment if films of various thickness have quantum well states at the same binding energy.[15] Because Φ only depends on energy, these two states must have identical phaseshifts. Their wave number is therefore given by

$$k=\pi(n_2-n_1)/(N_2-N_1)d \qquad (3)$$

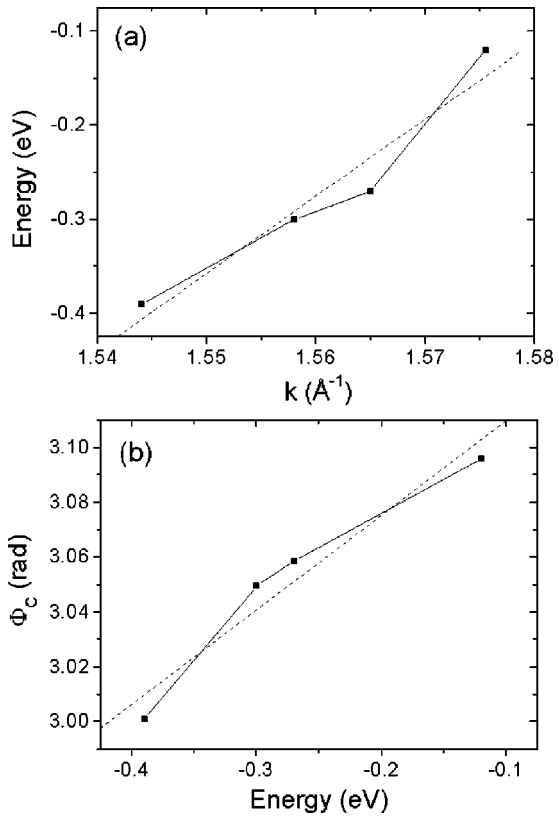

FIG. 3. (a) Experimental band structure $E(k)$ of Pb in the ΓL direction in the second Brioullin zone. The linear fit produces a k_F of 1.591 ± 0.006 Å^{-1}. (b) Experimental phaseshift Φ_C with linear fit.

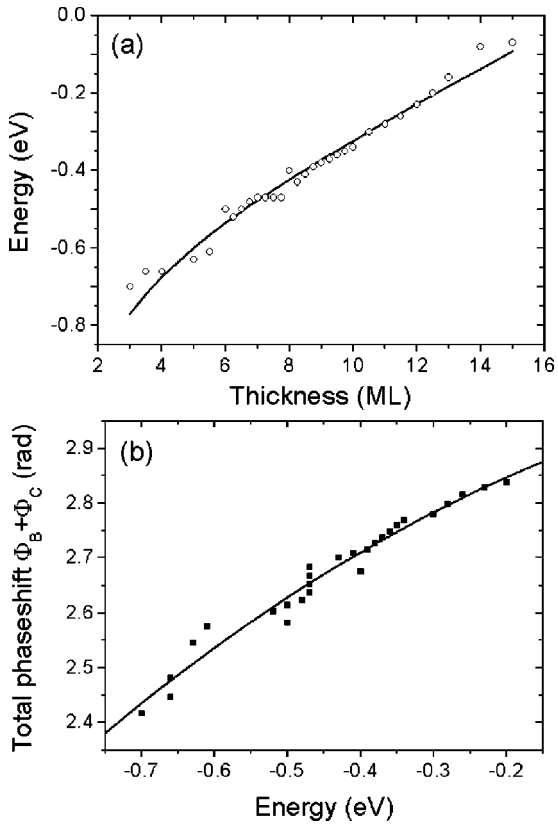

FIG. 4. (a) Measured quantum well energies for the $p=2$ branch (open circles) and the fit to the phase accumulation model. (b) Total phaseshift $(\Phi_B+\Phi_C)$ from the fit in (a).

with N_1 and N_2 corresponding to the number of layers in each film. This value for k gives, along with Eq. (1) the total phaseshift at that particular energy. Because the dataset is limited to a small energy window of only 0.7 eV, this analysis can only be implemented for four pairs of quantum well states. The result for $E(k)$ is shown in Fig. 3(a). The band structure is approximately linear for such a small interval. The fit gives a value for k_F of 1.591 ± 0.006 Å^{-1}, which is in very good agreement with De Haas-Van Alphen measurements[16,11] which produced a value of 1.596 Å^{-1}.

From the experimental relationship $k(E)$ and WKB values of Φ_B from Eq. (2), Φ_C can be calculated, which is a slowly varying function of energy. A linear fit gives the result $\Phi_C = a + bE$, with $a = 3.1 \pm 0.1$ rad and $b = 0.34 \pm 0.11$ rad eV^{-1}, as shown in Fig. 3(b). These values are similar to those of Al/Si(111),[17] Ag/Si(001) and Ag/Si(111).[18]

At low coverages (<8 ML) the finite square well model deviates significantly from the photoemission branches with $p=1$ and $p=2$. The square well model ignores the band structure and does not come anywhere close to reproducing the correct boundary conditions. The deviation from this model becomes increasingly important for thinner films. The phase accumulation model, instead, reproduces the photoemission branches over the entire coverage range. Figure 4(a) shows a fit to the $p=2$ photoemission branch using Eq. (1) in combination with the condition $n=(3N-p)/2$, assuming that the dispersion $k(E)$ remains linear down to 0.7 eV binding energy. Phaseshifts are shown in Fig. 4(b).

Figure 2(b) shows the photoemission intensity at the Fermi level as a function of Pb coverage. The values for this graph are obtained by symmetrizing the spectra.[19,20] In this procedure a spectrum (with $E_F=0$) and the spectrum with reversed energy sign are added up as shown in the inset of Fig. 2(b). This symmetrization procedure essentially removes the Fermi-Dirac distribution. The symmetrized intensity peaks when a state crosses the Fermi level. The vertical axis of Fig. 2(b) shows the height of the peak in the symmetrized spectrum devided by the height of the Fermi edge of a single spectrum (for normalization purposes). The broad features in Fig. 2(b) (i.e., the broad peaks around 9 and 16 ML) correspond to the Fermi-level crossing of the first ($p=1$) and second ($p=2$) photoemission branches of quantum well states. A quantum well state close to E_F gives rise to an increased intensity at E_F. The maxima of these peaks are indicated as filled circles in Fig. 2(a) and are situated where the photoemission branches would cross the Fermi level. The overall shape of Fig. 2(b) reflects the long-wavelength oscillation in the so-called "misfit function" $\delta = |Nd - n\lambda_F/2|$ which was introduced by Hinch *et al.*[1] Fermi-level crossings appear when $\delta = 0$, which happens when the coverage equals 9 and 16 ML. Pronounced dips in the photoemission intensity appear at 13 and 20 ML. At these points, the highest occupied quantum well state has the highest binding energy, i.e., these are the midpoints between two subsequent Fermi-

level crossings. With increasing coverage, the branches come closer together which explains the fact that the intensity minimum at 13 ML is deeper than the minimum at 20 ML.

The data in Fig. 2 of the paper by Su *et al.*[5] show the first Fermi-level crossing when the Pb islands grow 8 ML high above their wetting layer. Altfeder *et al.*[12] observe the crossing of the second branch ($p=2$) at an island height of 15 ML. Our data indicate Fermi-level crossings at 9 and 16 ML which shows that the wetting layer in the STM experiments[5,12] can only be one layer thick instead of three, as was claimed in these studies. Taking a wetting layer of only 1 ML, all of the quantum well energies measured in the STM/STS experiments[5,12] fit our photoemission results nicely. A 1 ML wetting layer reduces the quantum numbers of Su *et al.* by 3.

From purely electronic considerations, higher binding energies at $\mathbf{k}_\parallel=0$ imply larger stability,[13] which would then suggest that films of 13 ML and 20 ML, and films below ≈ 8 ML should be particularly stable. Realizing again that the spectra are not layer resolved and that the $p=1$ branch belongs to the odd-numbered layers, whereas the $p=2$ branch belongs to the even-numbered layers, it is immediately evident that below 9 ML, the even-numbered layers are more stable than odd-numbered layers, whereas the odd-numbered layers are more stable between 9 and 16 ML. Alternatively, below 9 ML islands consisting of an odd number of atomic layers above the wetting layer should be more stable than those with an even number of atomic planes. STM[21] and spot profile analysis LEED data[6] indeed suggest that 5 ML and 7 ML height islands are strongly preferred; however, the strongest preference for 7 ML height islands is inconsistent with the increased binding energy of the $p=2$ branch towards lower coverage. The strong dips at 13 ML and 20 ML call for STM investigations to explore the possibility of a preferred thickness in this coverage range.

B. Angle-resolved photoemission

The in-plane dispersion of a quantum well state at 0.30 eV binding energy ($p=2$) of a 9 ML Pb film is measured with angle-resolved photoemission spectroscopy. The spectra are recorded at a temperature of 120 K. The data for the two main crystallographic directions ΓM and ΓK are plotted in Fig. 5.

The parallel momentum $\mathbf{k}_\parallel$ was obtained from $\hbar\mathbf{k}_\parallel = \sqrt{2mE_k}\sin\theta$, with $E_k = h\nu - E_b - \phi_a$, and ϕ_a the work-function of the analyser. The values for the effective masses m^* derived from the spectra in the ΓM and ΓK direction are $3.95m_e$ and $3.61m_e$, respectively. To check whether these high values of the effective mass are an intrinsic property of two-dimensional Pb, DFT calculations have been performed on free standing Pb films, according to the localized spherical wave technique.[22] This method is a modification of the augmented spherical wave program that was developed by Williams *et al.*[23] Exchange and correlation were treated within the local spin-density approximation and scalar relativistic effects were included.[24,25] The lattice of Pb atoms was not allowed to relax in the calculations. The effective masses from the calculations are listed in Table I.

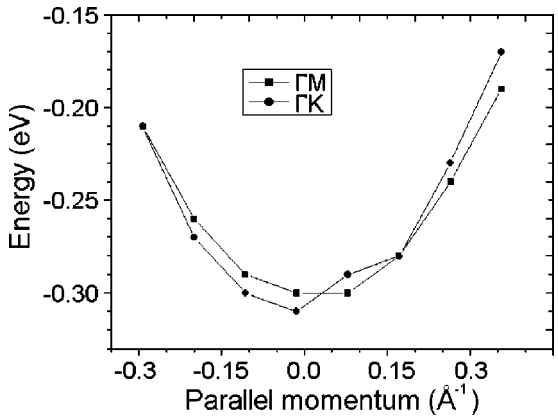

FIG. 5. Parallel dispersion of a 9 ML Pb film on Si(111)7×7 in the ΓM and ΓK directions. The effective masses are 3.95 and 3.61, respectively.

These theoretical values of m^* show numbers from 0.6 to $1.3m_e$ and an increase of the effective mass with decreasing binding energy. Similar behavior has been observed for Al/Si(111)[26] and Ag/Si(111).[27] From these numbers it is clear that the measured values for m^* cannot be attributed to the electronic properties of two-dimensional Pb. Other studies have indicated unexpected trends and sometimes unusually large mass parameters for quantum well states near the valence-band edge of the substrate. Examples include Ag on Si(001),[28] Al on Si(111),[26] and Ag or Cu on V(001).[29] For Pb on Si(111)7×7, the Fermi level is located near the bottom of the Si band gap[30] which means that the $p=2$ band of the 9 ML film must be close to the valence band maximum. We conjecture that this causes the unusually large values for m^*.

C. Influence of the photon energy

At 22 eV photon energy quantum well states can only be observed for binding energies <0.7 eV. However, if the photon energy is varied, quantum well states can be observed at different binding energies. For example, around $h\nu = 31$ eV a quantum well state appears at 3.3 eV binding energy. A series of photoemission spectra from a 4.5 ML Pb film on Si(111)7×7 taken with photon energies from 22 to 32 eV is presented in the gray scale plot of Fig. 6(a). This gray scale plot is obtained by multiplying the second derivative of the photoemission spectra with a function that corrects for the increased lifetime broadening at higher binding energy. This correction function is given by $-\sqrt{(\alpha E_b)^2+\Delta E_{instr}^2}$, with E_b the binding energy, ΔE_{instr} the instrumental energy resolution and $\alpha(=0.1)$ a constant to be adjusted to obtain good contrast in the entire energy range

TABLE I. Effective mass m^* (in units of m_e) as a function of binding energy (in eV) in the ΓM and ΓK direction from DFT calculations of Pb slabs.

Energy (eV)	4.03	3.36	2.54	1.39	0.16
$m^*(\Gamma M)$	0.59	0.65	0.78	0.89	1.28
$m^*(\Gamma K)$	0.60	0.62	0.64	0.86	1.01

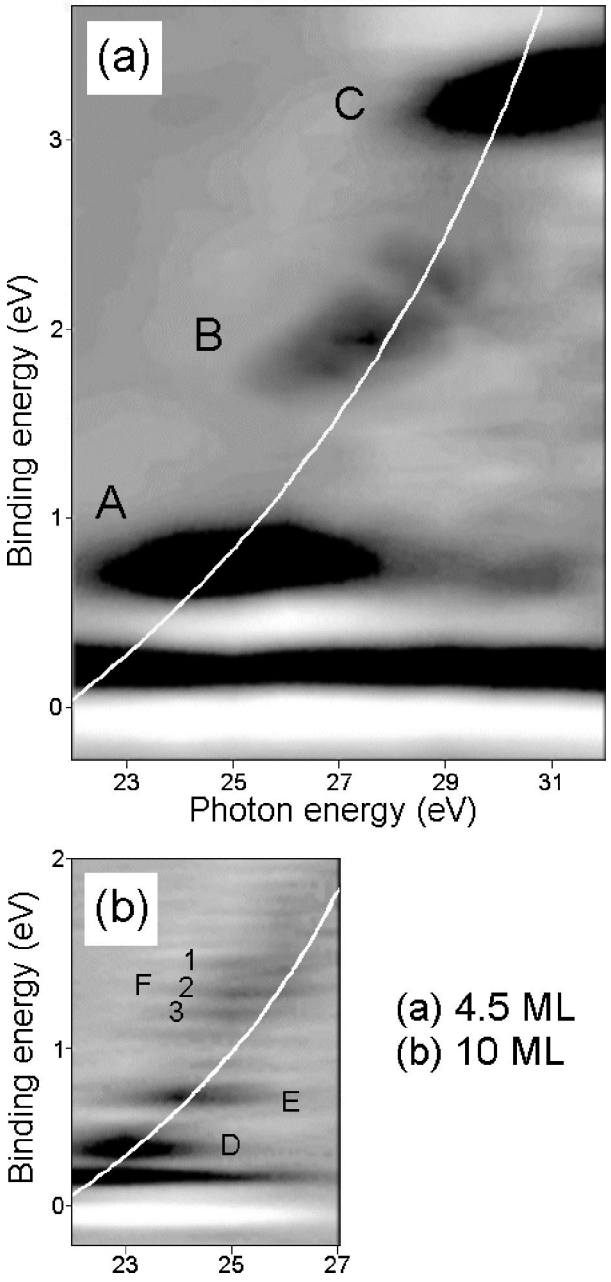

FIG. 6. Gray scale representation of the photoemission spectra from a 4.5 ML (a) and 10 ML (b) Pb film on Si(111)7×7 as a function of the photon energy. Black and white mean high and low photoemission intensity, respectively. The gray line indicates the dispersion of the bulk Pb *sp* band.

of the plot.[31] In this figure, black represents high photoemission intensity while white represents low photoemission intensity.

It can be clearly seen that the intensity of the quantum well state at 0.7 eV binding energy is diminished for photon energies >27 eV and that the state at 3.3 eV binding energy is only visible for $h\nu > 28$ eV. The quantum well state at 2.0 eV binding energy is less pronounced and only visible in the region between 26 and 29 eV. In this 4.5 ML Pb film, the state labeled *A* at 0.7 eV binding energy can be attributed to the $p=2$ branch, the state labeled *B* (1.9 eV binding energy) to the $p=3$ branch and state *C* (3.3 eV binding energy) to the $p=4$ branch. The contribution of the $p=1$ branch is observed in the raw spectra for photon energies from 22 to 25 eV, but it is not visible in the gray scale plot due to the strong curvature near the Fermi level.

For the 10 ML film of Fig. 6(b), states *D* and *E* at 0.3 and 0.7 eV binding energy can be attributed to the $p=2$ and $p=3$ branches, respectively. For binding energies greater than 1 eV, the individual quantum well states of the $p=4$ branch (1.1 to 1.5 eV binding energy) can be observed and are labeled $F1$–$F3$. From the simple finite square well model, one finds that the $F1$, $F2$, and $F3$ states correspond to different layer thickness (8, 10, and 12 ML, respectively), which is indicative of a rough growth front.

The observed intensity maxima of the quantum well states coincide with photon energies for direct transitions[32,33,28] in bulk Pb. The curves in Figs. 6(a) and 6(b) indicate the locations, where direct transitions would be possible in bulk Pb.[34] The valence states in ultrathin films are quantized, but the photoemission matrix elements do not deviate much from those in the bulk.[35,36] In thin films however, matrix elements only integrate over the film region, which causes a broadening in momentum (=energy) space.[37] This is illustrated in the Figs. 6(a) and 6(b). The photon energy range in which a certain quantum well state can be observed for a 10 ML film is 1.7 ± 0.1 eV [Fig. 6(b)] while for a 4.5 ML film it is 2.7 ± 0.3 eV [Fig. 6(a)].

IV. SUMMARY

The growth of Pb on Si(111) has been studied with photoemission spectroscopy. The experimental photoemission branches of quantum well states can be described with a reduced quantum number $p \equiv 3N-2n$. The number p can be viewed as a reduced quantum number corresponding to a long-wavelength modulation that satisfies the condition $p\lambda'/2=2Nd$. The photoemission branches reflect the general property of the Pb films that in the energy range of interest, each bilayer of Pb can support approximately three antinodes of the quantum well wave function. The photoemission branches cross the Fermi level when the condition $Nd=n\lambda_F/2$ is satisfied. The quantum well states are furthermore characterized by a large in-plane effective mass and strong matrix element effects for photo-ionization. The present study also sheds some light on previous STM experiments. It is now evident that below 9 ML, films with an even number of atomic layers are electronically more stable than those with an odd number of layers. This observation accounts for the fact that the ''magic'' islands in STM studies all have an odd number of atomic layers above the wetting layer. The wetting layer in the STM studies consists of only a single layer of Pb.

ACKNOWLEDGMENTS

The authors thank M.C. Tringides and M.Y. Chou for fruitfull discussions and T. Balasubramanian, C.D. Laman, and R. Staakman for technical assistance. This work has been financially supported by the Nederlandse Organisatie

voor Wetenschappelijk Onderzoek, gebied Chemische Wetenschappen (NWO-CW) and the European Union by supporting the MaxLab facility under Contract No. HPR1-CT-1999-00058. Oak Ridge National Laboratory is managed by UT-Battelle, LLC, for the U.S. Department of Energy under Contract No. DE-AC05-000R22725.

*Electronic address: a.mans@tnw.tudelft.nl

[1] B.J. Hinch, C. Koziol, J.P. Toennies, and G. Zhang, Europhys. Lett. **10**, 341 (1989).
[2] J. Braun and J.P. Toennies, Surf. Sci. **384**, L858 (1997).
[3] A.R. Smith, K.J. Chao, Q. Niu, and C.K. Shih, Science **273**, 226 (1996).
[4] K. Budde, E. Abram, V. Yeh, and M.C. Tringides, Phys. Rev. B **61**, R10 602 (2000).
[5] W.B. Su, S.H. Chang, W.B. Jian, C.S. Chang, L.J. Chen, and T.T. Tsong, Phys. Rev. Lett. **86**, 5116 (2001).
[6] V. Yeh, L. Berbil-Bautista, C.Z. Wang, K.M. Ho, and M.C. Tringides, Phys. Rev. Lett. **85**, 5158 (2000).
[7] Z.Y. Zhang, Q. Niu, and C.K. Shih, Phys. Rev. Lett. **80**, 5381 (1998).
[8] W.D. Knight, K. Clemenger, W.A. de Heer, W.A. Saunders, M.Y. Chou, and M.L. Cohen, Phys. Rev. Lett. **52**, 2141 (1984).
[9] B.N. Jensen, S.M. Butorin, T. Kaurila, R. Nyholm, and L.I. Johansson, Nucl. Instrum. Methods Phys. Res. A **394**, 243 (1997).
[10] H.H. Weitering, A.R.H.F. Ettema, and T. Hibma, Phys. Rev. B **45**, 9126 (1992).
[11] M. Jalochowski, H. Knoppe, G. Lilienkamp, and E. Bauer, Phys. Rev. B **46**, 4693 (1992).
[12] I.B. Altfeder, K.A. Matveev, and D.M. Chen, Phys. Rev. Lett. **78**, 2815 (1997).
[13] D.A. Luh, T. Miller, J.J. Paggel, M.Y. Chou, and T.-C. Chiang, Science **292**, 1131 (2001).
[14] G.E. McRae, Rev. Mod. Phys. **51**, 541 (1979).
[15] S.A. Lindgren and L. Walldén, Phys. Rev. Lett. **61**, 2894 (1988).
[16] J.R. Andersen and A.V. Gould, Phys. Rev. **139**, A1459 (1965).
[17] L. Aballe, C. Rogero, S. Gokhale, S. Kulkarni, and K. Horn, Surf. Sci. **482-485**, 488 (2001).
[18] A. Arranz, J.F. Sánches-Royo, J. Avila, V. Pérez-Dieste, P. Dumas, and M.C. Asensio, Phys. Rev. B **65**, 195410 (2002).
[19] M.R. Norman, H. Ding, M. Randeria, J.C. Campuzano, T. Yokoya, T. Takeuchi, T. Takahashi, T. Mochiku, K. Kadewaki, P. Guptasarma, and D.G. Hinks, Nature (London) **392**, 157 (1998).
[20] J. Mesot, M. Randeria, M.R. Norman, A. Kaminski, H.M. Fretwell, J.C. Campuzano, H. Ding, T. Takeuchi, T. Sato, T. Yokoya, T. Takahashi, I. Chong, T. Terashima, M. Takano, T. Mochiku, and K. Kadowaki, Phys. Rev. B **63**, 224516 (2001).
[21] M. Hupalo and M.C. Tringides, Phys. Rev. B **65**, 115406 (2000).
[22] H. van Leuken, A. Lodder, M.T. Czyzyk, F. Springelkamp, and R.A. de Groot, Phys. Rev. B **41**, 5613 (1990).
[23] A.R. Williams, J. K Cler, and C.D. Gelatt, Jr., Phys. Rev. B **19**, 6094 (1979).
[24] L. Hedin and B.I. Lundqvist, J. Phys. C **4**, 2064 (1971).
[25] M. Methfessel and J. K Cler, J. Phys. F: Met. Phys. **12**, 141 (1982).
[26] L. Aballe, C. Rogero, P. Kratzer, S. Gokhale, and K. Horn, Phys. Rev. Lett. **87**, 156801 (2001).
[27] I. Matsuda, T. Ohta, and H.W. Yeom, Phys. Rev. B **65**, 085327 (2002).
[28] I. Matsuda, H.W. Yeom, T. Tanikawa, K. Tono, T. Nagao, S. Hasegawa, and T. Ohta, Phys. Rev. B **63**, 125325 (2001).
[29] T. Valla, P. Pervan, M. Milun, A.B. Hayden, and D.P. Woodruff, Phys. Rev. B **54**, 11 786 (1996).
[30] D.R. Heslinga, H.H. Weitering, D.P. van der Werf, T.M. Klapwijk, and T. Hibma, Phys. Rev. Lett. **64**, 1589 (1990).
[31] T. Abukawa, M. Sasaki, F. Hisamatsu, T. Goto, T. Kinoshita, A. Kakizaki, and S. Kono, Surf. Sci. **325**, 33 (1995).
[32] T. Miller, A. Samsavar, and T.-C. Chiang, Phys. Rev. B **50**, 17 686 (1994).
[33] W.E. McMahon, T. Miller, and T.-C. Chiang, Phys. Rev. B **54**, 10 800 (1996).
[34] K. Horn, B. Reihl, A. Zartner, D.E. Eastman, K. Hermann, and J. Noffke, Phys. Rev. B **30**, 1711 (1984).
[35] E.D. Hansen, T. Miller, and T.-C. Chiang, J. Phys.: Condens. Matter **9**, L435 (1997).
[36] M. Milun, P. Pervan, and D.P. Woodruff, Rep. Prog. Phys. **65**, 99 (2002).
[37] A. Mugarza, J.E. Ortega, A. Mascaraque, E.G. Michel, K.N. Altmann, and F.J. Himpsel, Phys. Rev. B **62**, 12 672 (2000).